Functional Sub-regions for Optic Flow Processing in the Posteromedial Lateral Suprasylvian Cortex of the Cat

O. Brosseau-Lachaine, J. Faubert and C. Casanova

École d'optométrie, Université de Montréal, Montreal, Quebec, Canada

During locomotion, an observer sees a large and complex pattern of visual motion called optic flow. This phenomenon is characterized by elements in the environment accelerating and expanding as they move peripherally. In cats, previous studies have indicated that the posteromedial part of the lateral suprasylvian (PMLS) cortex may be involved in the processing of optic flow fields. We further addressed this issue by studying the importance of specific parameters of the optic flow patterns and investigating whether cell responses to these stimuli depend on receptive field (RF) location in the visual field. Results can be summarized as follows: approximately two-thirds of PMLS cells responded to optic flow fields and a subset of these (84/153) showed a clear direction selectivity for motion along the frontal axis. Of these units, the majority responded preferentially to expansion rather than contraction of the pattern. Cells' responses depend on RF location in the visual field. For centrally located RFs, tested both when the origin of motion was within the RF or at the area centralis, responses were generally comparable whether or not size or speed gradients were removed from the optic flow pattern. A different tendency was observed for peripherally located RFs. In general, these cells exhibited a preferred direction almost exclusively when the origin of motion was placed at the area centralis, and neuronal discharges and direction selectivity for many of them were reduced when the optic flow cues were removed from the pattern. The results of this study suggest that there may be functional differences in response properties between PMLS cells located in the central and peripheral parts of the visual field that may reflect a specialization of the PMLS cortex in optic flow processing.

Introduction

During locomotion in a structured environment, an observer sees a large and complex pattern of visual elements in motion. This perceptual phenomenon is commonly referred to as an optic flow field, and is usually characterized by cues such as the radial expanding motion of elements in the external world that are accelerating and increasing in size as the scene moves on the retina. It was first described by Gibson (Gibson, 1950), who emphasized its importance for the control of heading in self-motion and visual navigation.

Recently, several studies have addressed the neural basis of optic flow processing. In primates, neurons selective to the direction of optic flow stimuli have been found in the dorsal division of the medial superior temporal area (MSTd) (Saito *et al.*, 1986; Tanaka *et al.*, 1989; Tanaka and Saito, 1989; Duffy and Wurtz, 1991a,b; Orban *et al.*, 1992; Lagae *et al.*, 1994) and at a higher level, in area 7a and in the anterior division of the superior temporal polysensory cortex (Siegel and Read, 1997; Anderson and Siegel, 1999). In cats, neurophysiological and behavioral studies have indicated that an extrastriate cortical area, the posteromedial part of the lateral suprasylvian (PMLS) cortex, is likely to play a role in visual analysis during locomotion (Spear *et al.*, 1983; Morrone *et al.*, 1986; Rauschecker *et al.*, 1987; Krüger *et al.*, 1993; Sherk *et al.*, 1995) [but see Li *et al.* (Li *et al.*, 2000)]. This assumption was first based on the fact that there is a centrifugal organization of the preferred direction of PMLS receptive fields (RFs) (Hamada, 1987; Rauschecker *et al.*, 1987) and that neurons in this area respond to three-dimensional displays (Toyama and Kozasa, 1982; Toyama *et al.*, 1985; Akase *et al.*, 1998).

Recently, Sherk and her collaborators specifically studied the responses of lateral suprasylvian (LS) neurons to optic flow displays (Kim *et al.*, 1997; Mulligan *et al.*, 1997; Sherk *et al.*, 1997). These authors found that approximately two-thirds of LS cells responded preferentially to movies simulating locomotion through a plain covered with small balls, in comparison to displays composed of similar elements but containing motion only in a frontoparallel plane (Kim *et al.*, 1997). While all these studies provided important data regarding the involvement of PMLS in optic flow processing, they did not address fundamental issues such as the impact of stimulus spatial location within the visual field given that the properties of the optic flow fields vary with eccentricity.

To further investigate the possible involvement of PMLS cortex in optic flow processing, we have studied RF sensitivity in the anterior and posterior parts of the PMLS to large stimuli covering most of the animal's visual field, thereby more appropriately simulating natural conditions. These two PMLS regions can be functionally distinguished on the basis of visuotopic representation and the spatial extent of the cells' RF (Palmer *et al.*, 1978; Sherk and Mulligan, 1993). We investigated the effect of varying specific parameters of optic flow displays, such as perceived velocity and size gradients of the constituting elements on PMLS cell responses. We also determined whether the coding of these characteristics depends on the eccentricity of the cell's RF within the visual field. Preliminary results have been published elsewhere in abstract form (Brosseau-Lachaine *et al.*, 1998, 1999).

Materials and Methods

Animal Preparation

Twenty-five normal adult cats (2.5–3.5 kg) were used for this study. All animals were treated in accordance with the guidelines of the Canadian Council on Animal Care. The animals were premedicated with atropine (0.04 mg/kg) and acepromazine (0.5 mg/kg). General anesthesia was induced by inhalation of halothane (initially 5%, then reduced to 2%) in a mixture of N_2O and O_2 (50:50%). The heart rate and the O_2 blood saturation were constantly monitored with an oxymeter (Nonin). Surgical wounds and pressure points were infused with lidocaine hydrochloride (2%). The right cephalic vein was cannulated and a tracheotomy was performed.

The cat was then placed in a stereotaxic frame (D. Kopf) and was artificially ventilated (N_2O/O_2: 70/30% and halothane 0.5–1%). Throughout the experiment, the animal was infused with a solution of 5% dextrose in lactated Ringer's solution containing gallamine triethiodide

(10 mg/kg per h) to suppress muscular movements. The end-tidal CO_2 partial pressure was monitored (Normocap 200, Datex) and was maintained at 30–34 mmHg by adjusting the rate and the stroke volume of the respiratory pump (Harvard). The cat's rectal temperature was kept constant around 37.5°C with a feedback controlled heating pad. ECG and EEG readings were continuously monitored to assure proper anesthesia. Antibiotic (trimethoprim and sulfadiazine 15 mg/kg b.i.d., s.c.) was given on a daily basis. The eyes were protected using contact lenses of appropriate refractive power. Pupils were dilated with atropine sulfate (1%) and nictitating membranes were retracted with phenylephrine hydrochloride (2.5%). The optic discs were displayed by tapetal reflection (Pettigrew *et al.*, 1979) and plotted on a paper sheet covering a tangent screen placed at 57 cm in front of the animal. The position of the area centralis of each eye was calculated and plotted (Bishop *et al.*, 1962). Craniotomies were performed over the posterior part of the suprasylvian sulcus on both hemispheres, at Horsley–Clarke coordinates AP 7 to –2, and L 11–16.

Single Unit Recording

Extracellular recording were made with varnished tungsten microelectrodes (2–5 MΩ; A-M Systems) angled in a coronal plane ~40° with respect to vertical, and lowered down the medial bank of the suprasylvian sulcus. The exposed cortex was covered with warm agar over which wax was melted to create a sealed chamber. Neuronal activity was amplified, displayed on an oscilloscope, and played through an audio monitor. A window discriminator (WPI) was used to isolate single units from the overall signal and action potentials were constantly monitored using the software Axoscope (Axon Instruments). Digital signals were fed to an acquisition program (spike 2 v3.x, CED, Cambridge, UK) via an analogue digital interface (CED 1401 plus). The responses for each stimulus condition were recorded as peristimulus time histograms of 10 ms binwidth.

Visual Stimulation

Manually controlled stimuli projected onto the tangent screen were used to map and characterize basic RF properties such as direction selectivity and ocular dominance. Each unit was then quantitatively tested. The stimuli were generated with a Macintosh G3 computer (Pixx software v1.5x, SMR) interfaced with the acquisition system, and were rear-projected by a LCD projector (InFocus Systems) onto the translucent screen subtending 94 × 70° of visual angle (mean luminance 25 cd/m²). The image had a resolution of 6.8 pixels/degree and the refresh rate was 67 Hz. The screen (Da-Lite) was made of a precise optical coating applied to an acrylic substrate (Da-Plex) allowing for a display of high optical quality and uniform light diffusion. For all cells except those showing strong inhibitory surrounds, full-screen stimuli were displayed. The stimulus was otherwise restricted to the RF boundaries. Each stimulus presentation, including a blank screen (spontaneous activity) lasted 4 s and was repeated five times or more. Presentations were pseudo-random and in most cases only the dominant eye was stimulated. Control recordings indicated that responses to optic flow fields were similar whether the pattern was presented monocularly or binocularly (*t*-test, $P > 0.05$). In addition, for binocular cells, casual observation did not reveal any differences in optic flow properties between the two eyes.

Conventional Stimuli

Sinusoidal gratings (60% contrast) drifting in the frontoparallel plane were first used to evaluate the general properties of the units, such as optimal orientation and preferred spatial and temporal frequencies. Directional selectivity was determined by varying the grating's direction of motion over 360° in 12 steps of 30°. Direction selectivity was also tested using random dot kinematograms drifting in a frontoparallel plane. The cell's direction selectivity was quantified by a direction index (DI) as follows:

$$DI = 1 - \frac{\text{response in the non-preferred direction} - \text{spontaneous activity}}{\text{response in the preferred direction} - \text{spontaneous activity}}$$

An index value of >0.5 indicates that the cell was selective for the direction of stimulus motion (Minville and Casanova, 1998). A value of >1 means that the firing rate for the non-preferred direction was below the spontaneous activity level.

We quantified the axial direction preferences (Rauschecker *et al.*, 1987) for each cell by computing the difference between the cell's preferred direction (as determined by gratings), and the polar angle of the RF center (defined as the angle of the RF center in polar visual field coordinates). A difference of 0° would indicate a preferred direction equal to the polar angle, suggesting a centrifugal preference (i.e. away from the center of gaze). A 180° difference between the polar angle and the preferred direction would correspond to a preference towards the center of gaze (centripetal motion).

Optic Flow Stimuli

We used a variety of stimuli to characterize the cells' sensitivity to optic flow (see Fig. 1). In the first part of the study, expanding (outward radial motion) or contracting (inward radial motion) circular sinusoidal gratings were presented. Also, radial sinusoidal gratings, rotating clockwise or counterclockwise were used. For these two stimuli, responses as a function of spatial and temporal frequencies were studied. The cell's direction selectivity (e.g. expansion versus contraction) was determined and quantified as previously described using the DI.

We subsequently presented more complex stimuli consisting of white elements distributed on a dark background with radial trajectories (outward, expansion or inward, contraction) from the origin of motion. These stimuli simulated the experience of a cat traveling down a 0.57 m diameter straight tunnel with elements along the walls, at a speed varying in most cases between 1 and 6 m/s. This range corresponds to the observed speeds of trotting and galloping cats (Goslow *et al.*, 1973; Halbertsma, 1983; Smith *et al.*, 1993). The origin of motion represented the aperture at the end of the tunnel, which was ~2° in diameter (Fig. 1*A*). In this simulated environment the comprising elements represent rectangles elongated in the dimension parallel to the tunnel's axis with a fixed physical width and length of 2 and 28.5 cm, respectively. The rectangles thus increased in size as they moved towards the periphery of the display (closer to the observer, see Fig. 1*A*). They subtended 0.2 × 0.2° at the origin of motion, and reached 1.3 (Width) × 4.4° (Length) at 20° eccentricity, and 3.8 × 22.7° ($W \times L$) at 50° of eccentricity (defined at the center of the rectangles). Elements had a projection profile where their size and speed increased with the square of the distance. Element velocity (s, in degree/s) at a given eccentricity was computed from the formula:

$$s = [((\sin(d))^2/r) \times s'] \times 180/\pi$$

where d is the distance of the element from the center of expansion (in degrees), r is the tunnel radius (in m) and s' is the physical speed of the cat (in m/s). For example, in this model, for a cat speed of 4 m/s, elements located at 5, 20, and 50° of eccentricity will have a velocity of 6, 90 and 450 degree/s respectively.

In order to evaluate the contribution of changes in element size to optic flow analysis, dots of fixed size whose movement followed the same projection profile as defined above (see inset in Fig. 8) were presented for a number of PMLS neurons. These dots had a constant size diameter that was generally set between 1 and 6° of visual angle. For a second subset of cells, we investigated the effect of removing the speed gradient on the cells' responses, so the elements moved at a constant speed. The effect of varying the spatial extent of the stimulus was investigated by comparing full field pattern responses to those when the stimulus was confined to the RF. Finally, the origin of motion was located either at the area centralis or within the center of the RF. In this study, the stimuli were always presented at 100% coherence as pre-testing with patterns of lower coherence did not elicit robust responses.

Statistical Analysis

Response properties computed from gratings and optic flow patterns were compared using paired Student's *t*-tests (significance level of 0.05) and the relationship between groups was assessed using the Pearson product-moment linear correlation. Uniformity of cell distribution within each response property was tested with a chi-square (χ^2) test.

Histological Analysis and Localization of Recording Sites

Electrolytic lesions were made along recording tracks (5 μA for 4 s). The animal was killed with an intravenous overdose of pentobarbital sodium (Euthanyl: 0.96 mg/kg) and the brain was fixed in a solution of buffered

formalin (10%). The cortex was cut in 60–70 μm thick sections in a coronal plane with a Vibroslice and these were stained with Cresyl Violet. The lesions were located under binocular viewing, electrode tracks were reconstructed with an image analysis system (MCID), and the laminar position of the recorded cells was established. All cells were located in the PMLS cortex as defined by Palmer *et al.* (Palmer *et al.*, 1978).

Results

General Observations

A total of 240 cells were recorded in the PMLS cortex. Of these, 153 units were quantitatively tested for the purpose of this study. The remaining cells were either poorly visually responsive, exhibited a high level of response variability, or were lost before the completion of the tests. The general properties of the analyzed units were typical of those reported previously in this area (Spear and Baumann, 1975; Camarda and Rizzolatti, 1976; Morrone *et al.*, 1986; Blakemore and Zumbroich, 1987; Gizzi *et al.*, 1990a,b; Dreher *et al.*, 1996; Minville and Casanova, 1998). For instance, the vast majority (83%) of units were direction selective to the frontoparallel motion of a sine-wave grating [mean DI of 0.85 ± 0.03 (SE)]. The mean optimal spatial frequency was 0.18 ± 0.01 cycles (c)/degree and the majority (68%) had a band-pass tuning profile (mean of 1.95 ± 0.06 octaves), with the remaining 32% exhibiting low-pass tuning functions. Most units had RFs located in the contralateral visual field within –6 to +80° in azimuth and –40 to +15° in elevation with respect to the area centralis. Ninety-five RFs were located in the binocular part of the visual field (up to ~40° of eccentricity) and 58 in the monocular part (from ~40 to 90°) [see Orban (Orban, 1984)].

Responses to Optic Flow Stimuli

Overall, the majority of PMLS cells (105/153; 68.6%) were sensitive to optic flow stimuli used in the present study. For the remaining units (48/153), we were unable to elicit any reliable responses with the available stimuli. No significant differences were observed between these two cell groups with respect to their basic properties [e.g. RF size and location, optimal spatial and temporal frequencies and corresponding bandwidth (*t*-test, $P > 0.05$)]. For most optic flow sensitive neurons, the maximal discharge rate was generally higher for sine-wave gratings than for optic flow stimuli. Furthermore, neurons sensitive to optic flow displays were often found in clusters.

Figure 1 shows the selectivity of all PMLS cells as a function of the three stimuli presented. The overall data were pooled in that no distinction was made regarding the location of the RF or the origin of the stimulus motion. Figure 1*A* shows the distribution of response profiles to expanding and contracting fields of dots. Ninety-two neurons out of 142 (64.8%) responded to stimulus motion and most of them (73/92, 79%) responded preferentially to a given direction of motion that corresponded, in almost all cases, to the expansion of the stimulus. Comparable results were obtained when the units were classified on the basis of their responses to circular gratings (Fig. 1*B*). The smaller proportion of direction selective cells (16/78, 21%) for this stimulus as compared with that with the dot pattern (Fig. 1*A*) may have occurred because the origin of motion of the circular grating was always within the RF (see below). Finally, a subset of 58 PMLS cells was also tested for their sensitivity to radial grating patterns (Fig. 1*C*). A small proportion of neurons (14/58, 24%) responded to this stimulus and very few cells were direction selective to either counter or clockwise directions of motion (six units).

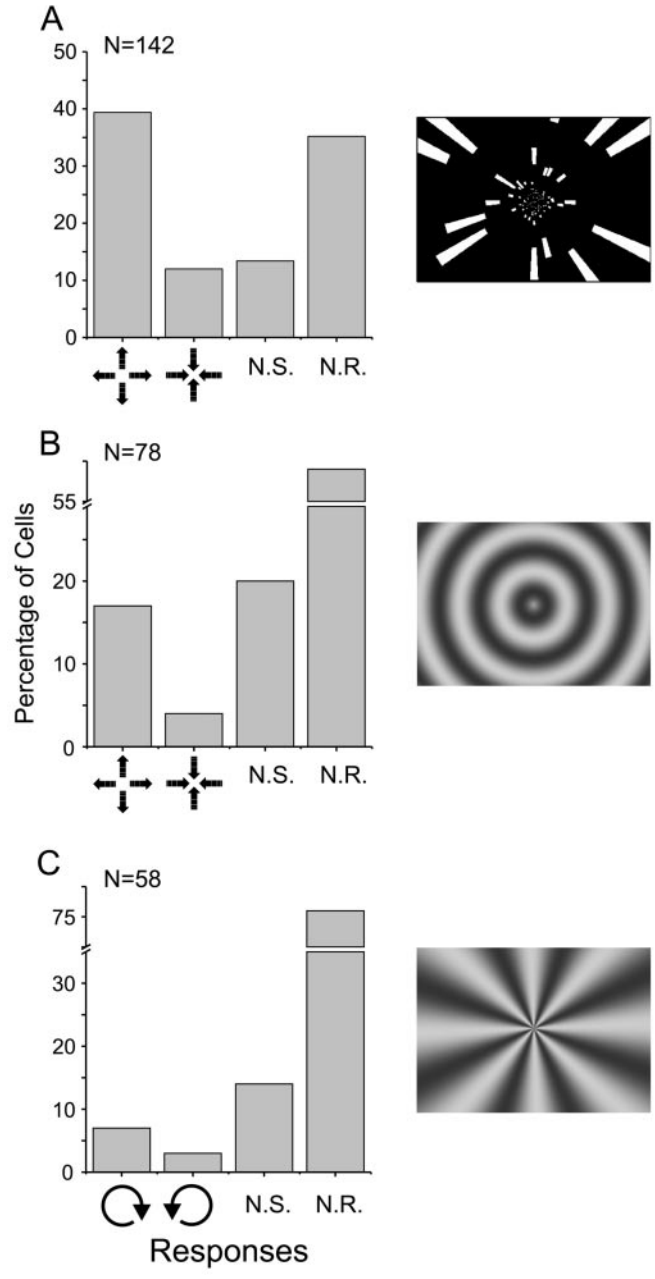

Figure 1. Distribution of the response profiles of all PMLS units as a function of the stimulus presented: (*A*) expanding or contracting elements, (*B*) circular gratings, (*C*) radial gratings. In (*A*) and (*B*), the arrow symbols represent the subsets of cells selective to a given direction of motion: outward and inward arrows illustrate expansion and contraction, respectively. In (*C*), circular arrows represent clockwise and counter clockwise motion. N.S. indicates optic flow sensitive cells that were not selective to the direction of motion. N.R. represents cells that did not respond to that particular stimulus.

None of these units were direction selective for expanding or contracting stimuli.

Centrally Located RFs

A total of 95 units had RFs located in the binocular zone of the visual field (between –6 and 40° in azimuth, and –23 and 10° in elevation). The vast majority of them were located between –2 and 25° in azimuth and –13 and 7° elevation. The mean ± SE RF

area was 252 ± 24.8 degree^2. There was no relationship between the responsiveness to optic flow and RF size (*t*-test, $P > 0.05$). We will refer to this group as neurons with central RFs.

Responses to Circular Gratings

Expanding and contracting circular gratings (see Fig. 1*B*) were first used to simulate motion in the frontal axis. Responses were studied as a function of spatial frequency to determine whether the spatial characteristics of PMLS units computed from expanding or contracting circular gratings were similar to those derived from translating gratings. Examples of spatial frequency tuning curves are shown in Figure 2. Most cells responded to circular gratings with a band-pass tuning profile (Fig. 1*A*, open circles) and the remaining units were of low-pass type (Fig. 1*B*, open circles). As a general rule, the optimal spatial frequency and tuning profile computed from circular (unfilled symbols in Fig. 1*A*,*B*) and frontoparallel gratings (filled symbols) were comparable. Figure 1*C* shows the relationship between the optimal spatial frequencies for both stimuli. Most of the data points are distributed along the regression line (slope = 1) with some scatter. The mean values ± SE for circular gratings and frontoparallel gratings were not significantly different (0.18 ± 0.03 and 0.21 ± 0.03 c/degree, respectively; *t*-test; $P > 0.1$). Comparison between the spatial frequency bandwidths also showed that almost all neurons exhibited the same level of selectivity for the two stimuli (mean of 2.1 ± 0.24 and 1.85 ± 0.13 octaves for circular and frontoparallel gratings, respectively, *t*-test, $P > 0.1$).

Responses to Fields of Elements

The optic flow sensitivity of most PMLS units was further characterized using expanding and contracting fields of elements. We first investigated whether the discharges of the neurons depended on the density of the elements constituting the pattern. A representative example is shown in Fig. 3*A–B*. Increasing the density of the elements yielded a rapid saturation (plateau) of the cells' responses for patterns with >75 elements. This behavior was observed for more than half of the units tested (14/26). Of the remaining 12 PMLS cells, five units were band-pass tuned for element density (mean optimal element number ± SE of 150 ± 42) and seven exhibited a low-pass tuning profile (mean optimal element number of 75 ± 19, with a mean number to evoke the half-maximum response of 155 ± 20 elements).

We subsequently studied the effect of varying the relative velocity of the optic flow pattern (Fig. 3*C*,*D*) by increasing the distance each element traveled. Most units (11 of 16) responded preferentially to low velocities, generally between 5 and 50 degree/s, and increasing the relative speed yielded a decrease in discharge rate (low-pass type). Among the five other units, one was characterized by a band-pass tuning function (optimal velocity of 14.3 degree/s, computed at the lateral edge

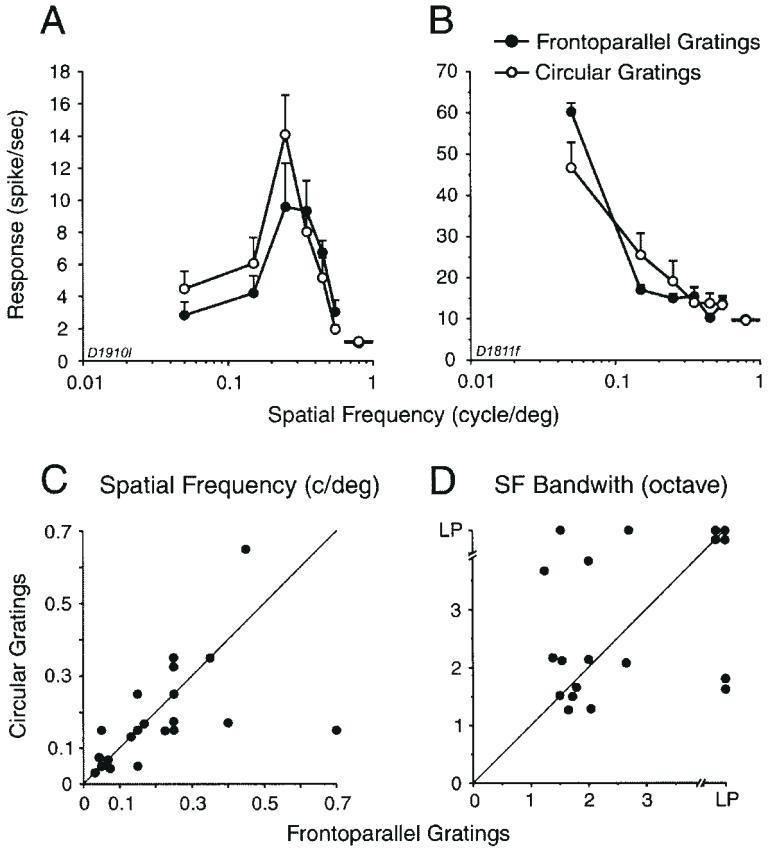

Figure 2. Responses of PMLS cells as a function of the spatial frequency for frontoparallel and circular gratings. Responses of a band-pass cell (*A*) and a low-pass tuned unit (*B*) are shown as tuning curves. Symbols on the right represent spontaneous discharge rates. Note that the response profiles are similar for both stimuli. (*C*) and (*D*) illustrate the relationship between optimal spatial frequencies and corresponding bandwidths computed for circular gratings and frontoparallel gratings, respectively. Most points are aligned near the diagonal line representing a perfect correlation (slope = 1) with some scatter. Note that the change in tuning of four cells in (*D*) (band-pass in one condition and low-pass in the other) should not be considered as a significant modification because responses to low frequencies for both conditions differed only slightly, but this difference was sufficient to permit the calculation of a tuning width for one stimulus but not the other.

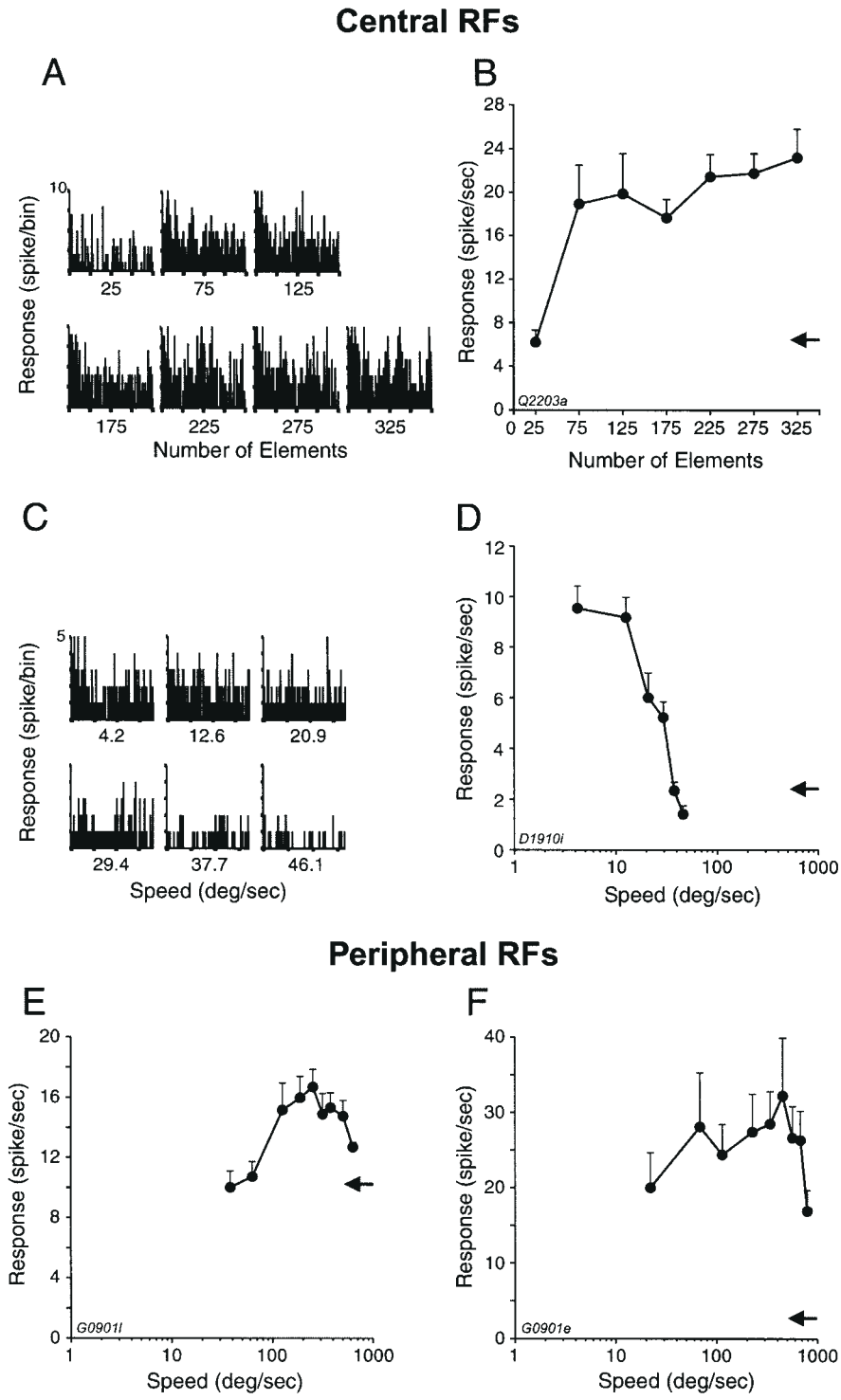

Figure 3. (*A–D*) Responses of PMLS cells with central RFs to the presentation of expanding elements, as a function of the number of elements in the pattern (*A* and *B*) and as a function of relative velocity (degree/s) (*C* and *D*). Results are shown in post-stimulus time histogram (PSTH) form (duration 4 s) and corresponding tuning curves. (*E* and *F*) Responses of two cells with peripheral RFs as a function of pattern velocity. Arrows to the right side of the graphs indicate spontaneous activity level. Errors bars represent SEMs.

of the RF), while the responses of the remaining four neurons were not attenuated at the higher velocities used.

Influence of the Origin of Motion

The effect of shifting the origin of motion of the pattern from the RF center to the area centralis was examined for a subset of 54 PMLS cells. In that condition, a total of 30 units responded to the motion of the optic flow pattern and 25 of these were selective to either the expansion (19 cells) or the contraction (six cells) of the stimulus (Fig. 4*A*, unfilled bars). The remaining five neurons were classified as non-selective. Figure 4 also shows the distribution of the cells' responses when the origin of motion was within the RF (filled bars). In both conditions there is a clear preference for stimulus expansion. However, the proportion of

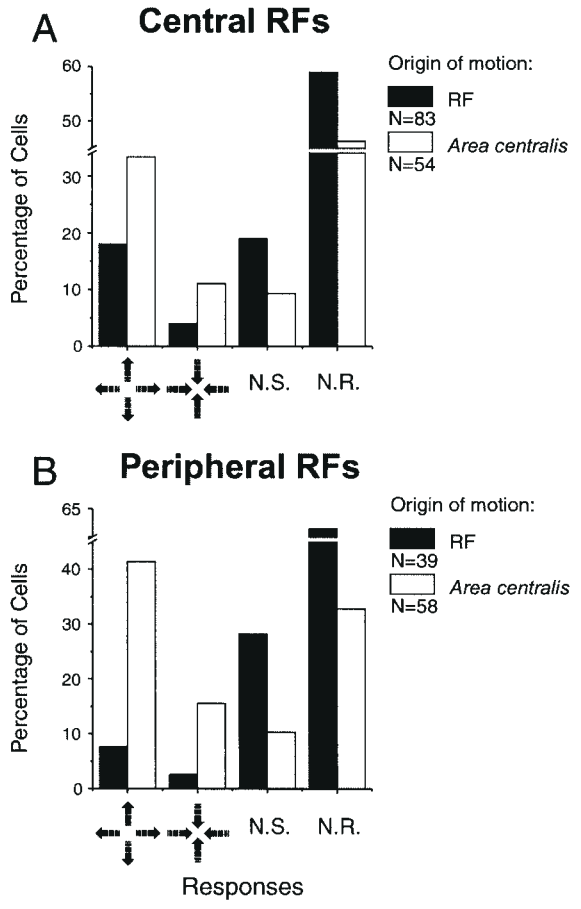

Figure 4. Distribution of the response profiles of centrally located (*A*) and peripherally located (*B*) PMLS cells tested with fields of expanding or contracting elements with the origin of motion either within the RF (solid bars) or at the area centralis (empty bars). The outward and inward arrows represent the subsets of cells selective to expansion and contraction, respectively. N.S. indicates optic flow sensitive cells with no preferred direction. The units that did not respond to any condition were classified as 'non-responsive' (N.R.).

direction-selective units was greater when the origin of motion was positioned within the area centralis, and consequently the number of non-selective and non-responsive units was decreased. It was observed that a number of cells (18 units) that could not be stimulated when the pattern motion was centered within the RF could be driven when the origin of motion was in the area centralis. Examples showing that the response profile of a given cell may vary according to the location of the origin of motion are shown in Figure 5. In Figure 5*A*, the cell responded in both conditions but was either considered as non-selective for expansion, when the origin of motion was in the RF and as expansion-selective when it was in the area centralis. Figure 5*B* illustrates the neural activity of a cell that only responds when the origin of motion was located at the area centralis. These responses could not be predicted on the basis of RF eccentricity, area, nor direction tuning width (*t*-test; $P > 0.05$). However, it is worth pointing out that in the two examples, the direction of the elements was roughly similar to the preferred direction (arrows) of the cells defined by stimuli moving in the frontoparallel plane.

Figure 6 shows the distribution of the axial direction preferences of the units that responded to the expansion of flow patterns originating from the area centralis (filled bars). Data in Figure 6*A* are grouped around 0 (see Materials and Methods),

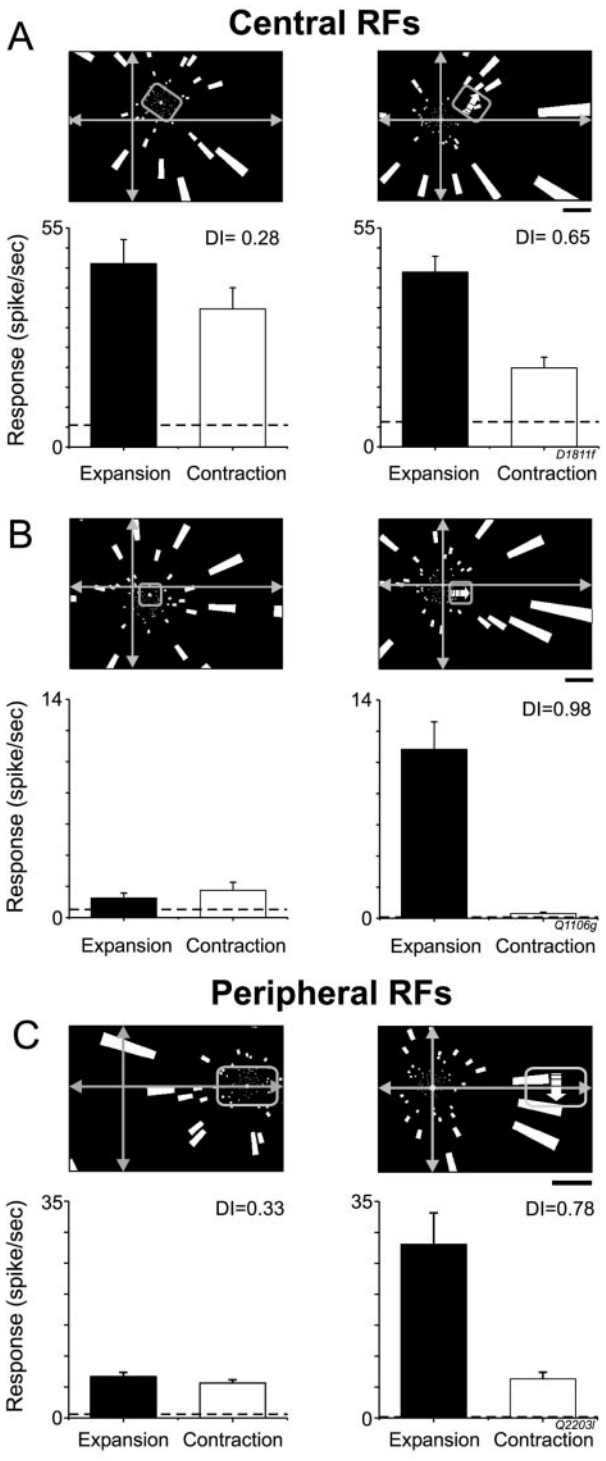

Figure 5. Responses of centrally located RFs when tested with expanding (filled bars) or contracting elements (unfilled bars) whose origin of motion was in the RF (left) and at the area centralis (right). (*A*) Example of a cell classified as non-selective when the motion originated from the RF, and selective for expansion when it was located at the area centralis. (*B*) This cell only responded when the motion originated within the area centralis. Note that in each example, there is centrifugal bias for direction. A single frame of the stimulus is shown on which is superimposed the location of the RF and the preferred direction in the frontoparallel axis (broken arrow). (*C*) Influence of the origin of motion on responses of cells with peripheral RFs. In the left diagram, the PMLS unit responded poorly and was not direction selective to elements originating from the RF center. The right drawing illustrates the responses of that same neuron when the origin of motion was moved to the area centralis. The unit then responded strongly and preferentially for the expansion of the flow field. Scale bars are ~20° and broken lines in the bar graphs represent spontaneous activity levels.

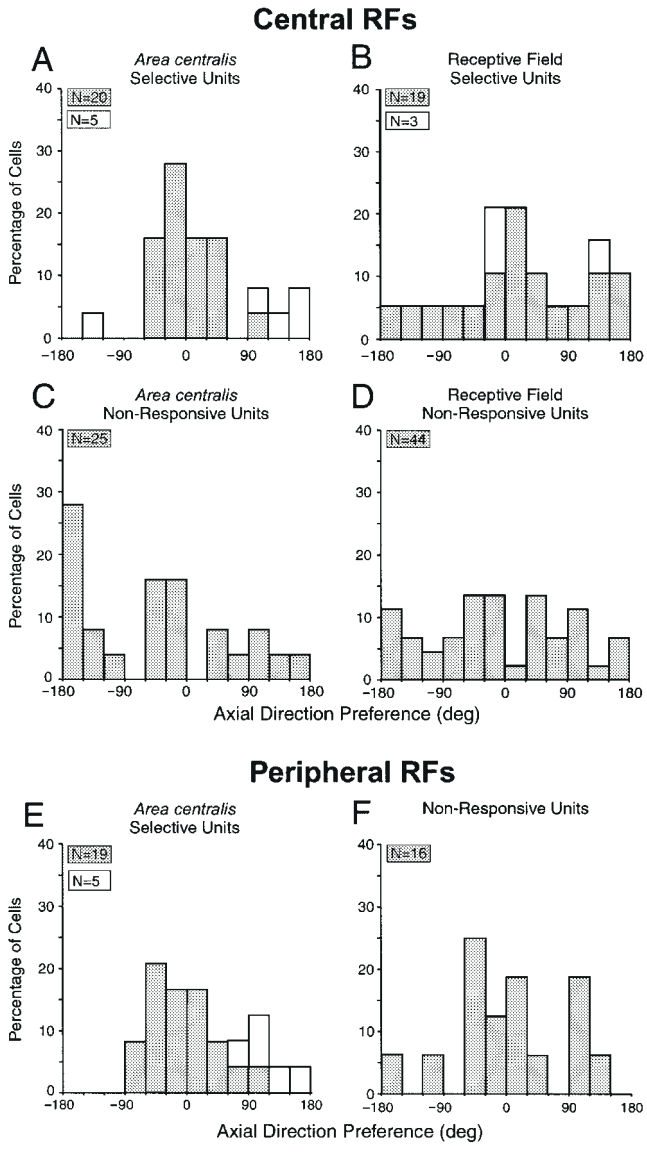

Figure 6. Distributions of axial direction preferences. (*A–D*) Cells with central RFs that were direction selective (*A* and *B*) or non-responsive (*C* and *D*) when tested with expanding and contracting elements with origins within the area centralis and the center of the RF, respectively (*A*) and (*B*). In (*A*), one contraction selective unit was not represented in the graph because the center of its hand-mapped RF nearly coincided with the area centralis. Therefore an axial preference could not be computed with confidence. (*E* and *F*) Neurons with peripheral RFs. Cells in (*E*) were direction selective to optic flow stimuli centered on the area centralis, and cells in (*F*) did not responded to optic flow patterns. In (*A*), (*B*) and (*E*), solid and open bars represent the axial direction preference for expansion- and contraction-selective cells, respectively.

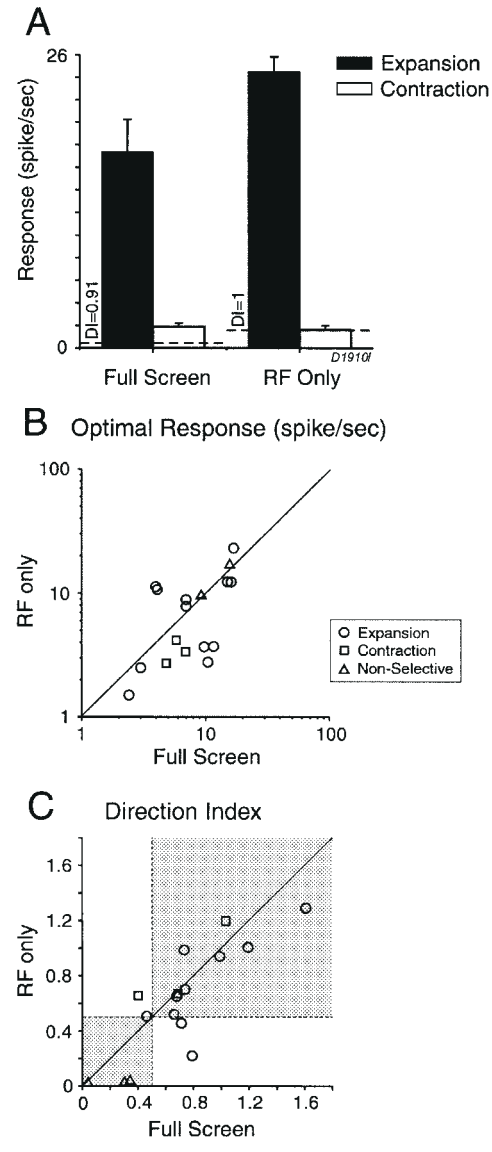

Figure 7. Responses of a PMLS cell as a function of the spatial extent of the stimulus (full screen or confined to the RF). (*A*) Response to the stimulus (field of elements) during expansion (filled bars) and contraction (unfilled bars) are shown in the bar graphs. Responses were not significantly different (*t*-test, $P > 0.05$). Broken lines represent spontaneous discharge rates. (*B*) The correlation between response strength when the stimulus was either confined to the RF or was presented as a full-screen pattern. For a number of cells (right side of the line of perfect regression), the response strength was greater for full-screen displays. (*C*) The relationship between the directional indexes in both conditions, for expansion (circles) and contraction (squares) selective units and for non-selective cells (triangles). Note that the majority of the points are skewed close to the line of perfect regression. The shaded areas contains cells for which direction selectivity was unaffected by stimulus size.

suggesting that these units' selectivity for stimulus expansion could be related to their axial direction preference. In support of this conclusion, the distribution of values for non-responsive cells is more uniform (Fig. 6*C*). The relationship between axial direction preferences and optic flow responses is less pronounced for cells that exhibited a direction selective response to the pattern when the origin of motion was within the RF (Fig. 6*B*). Figure 6*D* shows the distribution of values for cells that did not respond when the origin was in the RF.

Influence of Stimulus Size

Given that units with centrally located RFs could respond when the origin of motion was within the RF, we investigated whether optic flow responses could be evoked when the stimulus was confined to the RF for a subset of 17 cells. An example is shown in Figure 7*A* as bar graphs. The discharge rates and the computed DIs were comparable across both conditions. The overall data are presented in Figure 7*B*,*C*. While many cells had higher response rates for large sized displays (data points on the right side of the perfect regression line), there was still a correspondence between the response strength computed in both conditions ($r = 0.66$, $P < 0.005$) as well as for the units' direction selectivity ($r = 0.83$, $P < 0.001$; mean DI ± SE of 0.74 ± 0.09 and

0.68 ± 0.12 for full screen and RF only conditions, respectively; *t*-test, $P = 0.35$). Thus, for centrally located RFs, comparable responses were obtained whether the area beyond the RF was stimulated or not.

Influence of Size Gradient

For 26 cells, we examined the effect of removing the size gradient of the optic flow pattern on response strength and selectivity (Fig. 8). Cells in Fig. 8*A*,*B* were stimulated with elements of increasing or constant size whose origin of motion was either in the center of the RF (open symbols) or at the area centralis (filled symbols). In both cases, the cells responded preferentially to the stimulus expansion with equal strength. Figure 8*C*,*D* further shows that removing the size gradient of the elements did not affect the direction selectivity nor the robustness of the responses of practically all neurons tested. There is a close relationship between the computed values as most data points are skewed around the line of perfect regression (origin of motion within the RF: $r = 0.91$, $P < 0.05$, and $r = 0.80$, $P < 0.05$ for the response strength and DIs, respectively. Area centralis: $r = 0.96$, $P < 0.05$, and $r = 0.89$, $P < 0.05$, for response strength and DIs, respectively).

Influence of Speed Gradient

The effect of removing element acceleration in the pattern was examined for a subset of 16 units. For most cells, removing this cue had little effect on responses of direction selective cells whether the origin of motion was within or outside the RF. An example is shown in Figure 9*A*. The cell responded preferentially to the expansion of the 'original' pattern. In the absence of acceleration, the discharges in the preferred direction were not affected and only a small reduction of the response in the non-preferred direction was observed. Comparison of the response strength and direction selectivity for all 16 cells in both conditions reveals that overall, cells having centrally located RFs are not strongly sensitive to the acceleration component of the stimulus (Fig. 9*B*,*C*). Despite some scatter, most data points (79%) are near the perfect regression line. For cells tested when the origin of motion was in the RF, overall mean responses ± SE (17.9 spike/s ± 5.6 and 11.5 spike/s ± 3.5, with and without acceleration, respectively) and direction selectivity indices (DIs of 0.59 ± 0.15 and 0.49 ± 0.18) were not significantly different (*t*-test; $P = 0.25$ and $P = 0.43$). Cells tested with elements originating from the area centralis exhibited mean response values that were comparable (13.8 ± 3.1 versus 10.4 ± 3.1 spike/s, for acceleration and constant velocity conditions, respectively; *t*-test; $P = 0.08$). No differences were observed for mean direction index values (DIs of 0.72 ± 0.11 versus 0.8 ± 0.07, with and without acceleration, respectively; *t*-test; $P = 0.63$).

Peripherally Located RFs

Cells with more peripherally located RFs (beyond 40°, in the monocular zone of the visual field) were encountered in the rostral part (between AP +4 and +7) of PMLS cortex and were generally more difficult to drive than those having centrally located RFs. Consequently, only 58 cells could be quantitatively studied. RFs were located between 40 and 83° (azimuth) and −42 and 14° (elevation) but the large majority had RFs between 40 and 74° (azimuth) and −23 and 12° (elevation). The mean RF ± SE area was 755 ± 58.1 deg^2. As for centrally located RFs, no relationship between the responsiveness to optic flow and RF size was noted (*t*-test, $P > 0.05$). This group will be referred to as neurons with peripheral RFs.

Responses to Optic Flow Stimuli

The overall optic flow sensitivity of PMLS cells with peripherally located RFs are presented in Figure 4*B*. Most of these neurons were either unresponsive or non-selective to the direction of motion when the origin of the flow pattern was within the RF (filled bars). However, a substantial number of cells responded unequivocally to the flow pattern (39 units) when the origin was moved to the area centralis (unfilled bars), and most of them exhibited a clear preference for a specific direction of motion (33 cells), corresponding in most cases to the expansion of the flow field (24 out of 33). The remaining 19 cells did not respond to optic flow stimuli.

A representative example is shown in Figure 5*C*. This PMLS neuron responded poorly to the expansion and contraction of a field of elements originating from the RF and did not exhibit any directional bias (left diagram). A different picture emerged when the origin of the pattern was shifted to the area centralis (right diagram). In that condition, the neuron responded vigorously to the expansion of the optic flow stimuli and strongly preferred stimulus expansion. Note that this unit had an axial direction preference of 90° (defined by translating gratings), i.e. roughly perpendicular to the centrifugal direction of the elements crossing the RF. This mismatch between the translation vector of the flow field and the translation direction selective RF was observed for seven other cells with peripheral RFs (axial direction preferences between 58 and 90°). Figure 6*E* illustrates the distribution of axial direction preferences for expansion-selective cells (filled bars). Overall, values are comparable to those obtained for cells with centrally located RFs (Fig. 6*A*). Figure 6*F* indicates that a proportion of cells that did not respond to the optic flow pattern also had centrifugal axial directional preferences.

As for cells with central RFs, we investigated the effect of varying the velocity of the optic flow pattern (Fig. 3*E*,*F*). Seven out of 11 units were characterized by broad band-pass tuning functions and responded to optimal velocities ranging between 140 and 500 degree/s (mean high cut-off ~1000 degree/s; Fig. 3*E*,*F*). Two other cells preferred lower speeds and their high cut-off ranged between 200 and 360 degree/s. The remaining two units responded equally to a very broad range of velocities and no attenuation of their discharges was observed for velocities up to 1000 degree/s.

Influence of Size Gradient

The influence of removing the size gradient was studied for a subset of 12 cells (10 selective for expansion, and two for contraction) with RFs located in the periphery of the visual field. For most units responding preferentially to stimulus expansion, neuronal discharges were enhanced when the elements increased in size (mean discharge rate ± SE for elements increasing in size: 13.2 ± 2 spike/s, for elements of constant size: 5.5 ± 0.9 spike/s; *t*-test; $P = 0.003$). This behavior is illustrated by the example depicted in Figure 8*E*. Despite the reduction of response strength when elements of constant size were presented, the preference for expansion was maintained (note that, for each cells, the size of the dots was varied to obtain a stimulus similar to that of the expanding elements constituting the original pattern). This occurred for most cells that responded preferentially for elements increasing in size. Figure 8*F* illustrates the relationship between response strength for the two conditions. The mean response amplitude for the two cells responding preferentially to stimulus contraction (squares) was not reduced by removing the size gradient.

Influence of Speed Gradient

The effect of eliminating the acceleration of the moving elements was investigated for 16 units (12 were selective for expansion and four for contraction). For many expansion-selective cells the absence of a speed gradient reduced the discharge rate in the preferred direction and consequently provoked a loss of direction selectivity. The strength of these changes increased with velocity, as shown in Figure 9*D*. In this example, the expansion-selective unit was stimulated with elements expanding from the area centralis for a range of speeds (upper bars). In the absence of acceleration (lower bars), the cell became less responsive and even failed to respond at 804 degree/s, a speed that still evoked responses when the acceleration was present. Comparison of the response amplitude in both conditions is shown in Figure 9*E* and reveals that expansion-selective PMLS cells tended to exhibit a higher degree of responsiveness when stimulated with accelerating elements rather than with elements moving at constant speed (mean ± SE of 11.6 ± 2 *s*/s and 5.4 ± 1.5 *s*/s, respectively; *t*-test, $P = 0.036$). Note that a subset of five cells was particularly affected by the manipulation of this

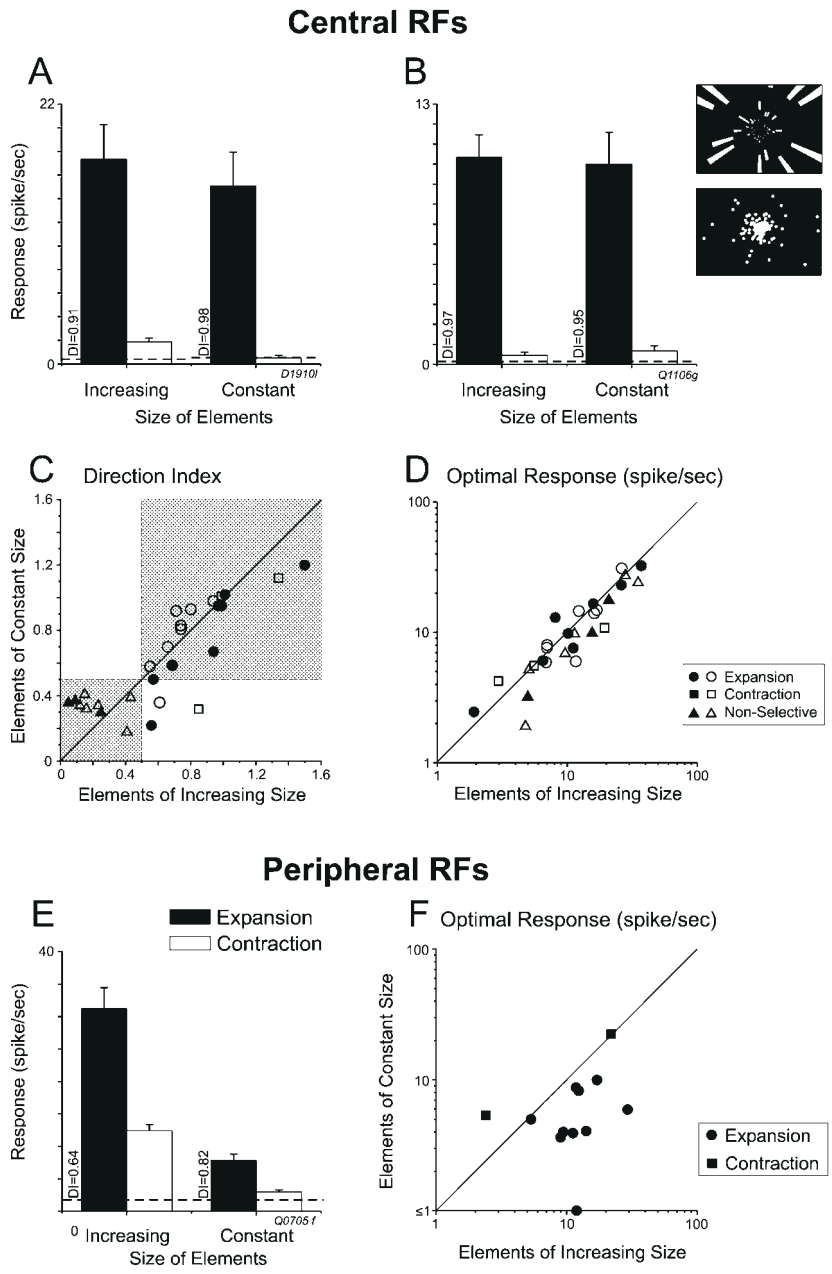

Figure 8. Influence of size gradient on optic flow responses. (*A–D*) Cells with central RFs. (*A*) and (*B*) illustrate examples of two expansion-selective units tested with elements of increasing or constant size, when the origin of motion was within the RF (*A*) or at the area centralis (*B*). The insets illustrate optic flow patterns with and without size gradient. (*C*) and (*D*) show the relationship between the directional indices and response strength computed from the responses evoked when the element size was kept constant or increased in size. Note that both properties were generally similar in both conditions as most points were distributed within the upper-right and lower-left quadrants (*C*, shaded areas) or near the line of perfect regression (*D*). Empty and solid symbols represent values computed when the origin of motion was in the RF and at the area centralis, respectively. (*E* and *F*) Neurons with peripheral RFs. (*E*) The discharges of a PMLS cell for elements increasing in size and for constant size elements. In both cases, the origin of motion was at the area centralis. (*F*) compares the response strength computed from the responses evoked when the size of the elements was kept constant or was increasing in size. Circles and squares represent expansion- and contraction-selective cells, respectively. In (*A*), (*B*) and (*E*), broken lines represent spontaneous activity levels.

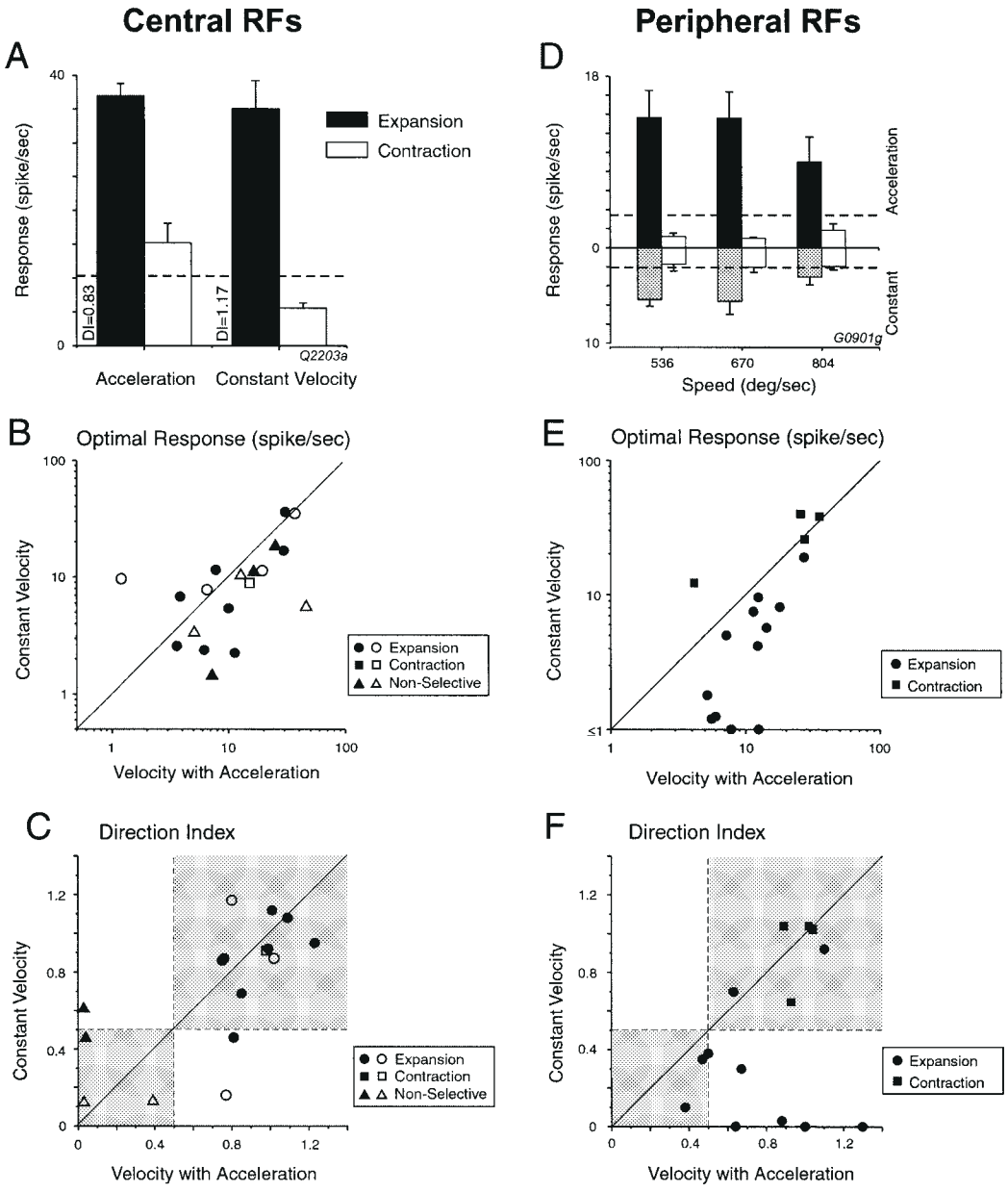

Figure 9. Influence of the acceleration of the pattern elements on the response profile. (*A–C*) Neurons with central RFs. (*A*) The response of a cell to expanding (solid bars) and contracting (open bars) elements when the latter are moving with or without acceleration. Broken lines represent spontaneous activity levels. (*B*) and (*C*) show the relationship between response strength and directional selectivity on the two velocity conditions. Unfilled and filled data points represent values computed when the origin of motion was in the RF and at the area centralis, respectively. Again, most points are close to the line of perfect regression with some scatter. (*D–F*) Neurons with peripheral RFs. (*D*) The response of an expansion-selective cell as a function of velocity. The response amplitude and direction selectivity was reduced when the stimulus velocity was constant. This effect was enhanced for increasing velocities. (*E*) and (*F*) show the relationship between response strength and directional selectivity with or without acceleration. In (*E*), all expansion-selective cells (circles) are located on the right side of the line of perfect regression. In (*F*), data points in the lower-right quadrant are close to the abscissa, indicating that the DI of these expansion-selective units were strongly affected when the acceleration factor was removed. However, this was not the case for contraction-selective cells (squares).

stimulus's parameter. One may note that the four contraction-selective units were not strongly affected by removing the acceleration component of the stimulus as was the case when the size gradient was removed. Figure 9*F* illustrates the finding that direction selectivity of a subset of cells (bottom-right quadrant) was reduced and even abolished by removing the speed gradient. Overall, direction selectivity indices (DIs of 0.81 ± 0.1 and 0.25 ± 0.1 with and without acceleration, respectively) were significantly different (*t*-test; $P < 0.001$).

Laminar Position

We assessed the laminar position for 82 centrally and 36 peripherally located PMLS units to determine whether there was a relationship between the responsiveness to optic flow field and the neurons' laminar position (Fig. 10). For both cell groups, there was no significant difference between the laminar distribution of optic flow sensitive (black and gray filled bars) and unresponsive cells (unfilled bars) ($\chi^2 = 6.3$, $P > 0.05$ and $\chi^2 = 2.1$, $P > 0.05$ for centrally and peripherally located RFs,

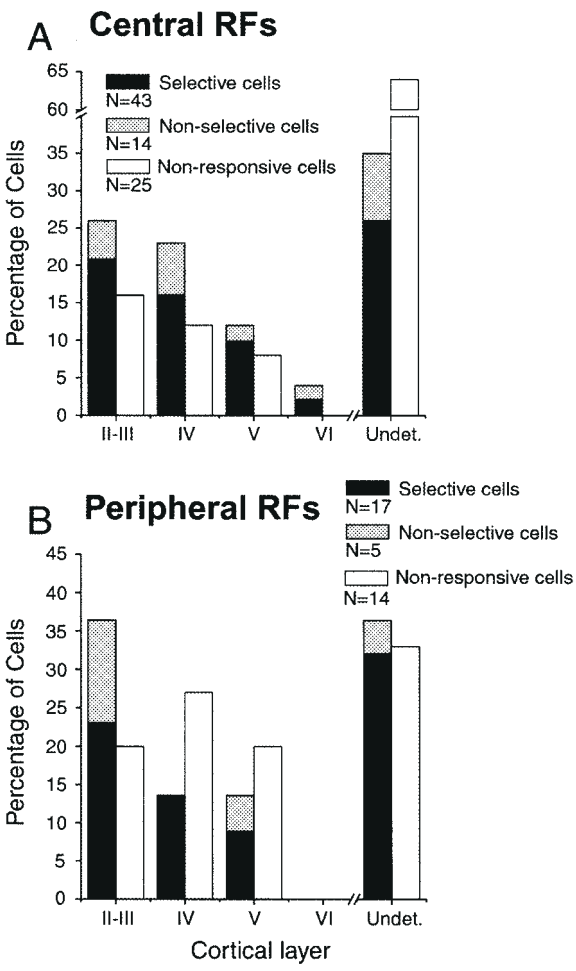

Figure 10. Laminar distribution of PMLS cells having RFs centrally (*A*) and peripherally (*B*) located. Black and gray filled bars represent optic flow selective and non-selective units, respectively, while unfilled bars represent unresponsive cells. For a number of neurons (Undet. group), we were unable to reconstruct the electrode tracks or identify the lesion marks so as to determine the location.

respectively). A higher proportion of peripherally located optic flow sensitive cells were found in cortical layers II–III, when compared with the laminar distribution of centrally located RFs. However, this tendency did not reach statistical significance ($\chi^2 = 2$, $P > 0.05$).

Discussion

Our results indicate that a majority of cells in the PMLS cortex respond to optic flow patterns, and that those exhibiting a direction preference respond preferentially to stimulus expansion (a condition that mimics the displacement of the visual scene during locomotion towards a target). More importantly perhaps is that our findings suggest that there may be a functional dichotomy within PMLS cortex on the basis of the response properties of centrally and peripherally located RFs. Central RFs could be driven by optic flow fields originating from the area centralis or within the RF and were, in general, poorly sensitive to specific optic flow cues. On the other hand, the majority of cells with peripherally located RFs only responded to a specific direction of motion when the origin of the flow field was placed at the area centralis and were more sensitive to cues such as size increment and element acceleration.

These findings are in agreement with the notion that PMLS cortex would be involved in the analysis of optic flow. Other groups have indeed found a bias for the radial-outward direction in cat area LS (Kim *et al.*, 1997) and comparable findings were described in primate area MST (Tanaka and Saito, 1989; Lagae *et al.*, 1994). This preference for stimulus expansion is also concordant with the original observations made by Hamada (Hamada, 1987) and Rauschecker *et al.* (Rauschecker *et al.*, 1987) that there is a centrifugal organization of direction preferences in the anterior region of PMLS cortex (Sherk *et al.*, 1995). Accordingly, we found that most expansion-selective cells having centrally located RFs with preferred directions away from the area centralis. Such a relationship was also present, but to a lesser extent, for cells with peripherally located RFs. In fact, a number of these neurons had a preferred direction defined by translating gratings perpendicular to that for the elements of the optic flow pattern (see example in Fig. 5*C*). Therefore these cells seem to extract the direction of the flow field from mechanisms other than a simple match between the RFs flow field and preferred axial vectors. One may propose the existence of sub-units within the RF that would not be tuned for the same direction of motion or that would be more sensitive to the oriented axes that characterize grating stimuli. Additional investigations are needed to test whether the sensitivity to moving stimuli varies across the RF.

The present study also reported that few PMLS cells were sensitive to rotating gratings. Only 24% of cells responded to these stimuli, and only half of these (10% of the whole population) were selective to a given direction of motion. This result differs somewhat from that reported in primates, where up to 20% of neurons in area MST were found to be direction selective for this type of motion (Lagae *et al.*, 1994). The fact that PMLS cells preferentially code radial rather than rotating motion might be related to the locomotion behavior of domestic cats versus that of monkeys when placed in a natural environment. Monkeys may frequently leap between tree branches (Lagae *et al.*, 1994) and young primates may get exposed to different flow fields early in life since the mother carries them. The primate visual brain may therefore be more likely to code for the rotation of the visual field, that could arise from changes in head axis during locomotion, than that of cats.

We generally found that neuronal responses and direction selectivity to optic flow stimuli of centrally located RFs was comparable when the pattern was restricted to the RF or covered a large portion of the visual field (see Fig. 7). This result was first surprising because, according to von Grünau and Frost, PMLS neurons exhibit a double-opponent process mechanism underlying their RF structure (von Grünau and Frost, 1983). In the present study, the nature of the dot pattern was such that the RF and its surrounding area were simultaneously stimulated by elements moving in non-corresponding directions. As a consequence, the surround inhibitory mechanisms, if direction selective [as suggested previously (von Grünau and Frost, 1983); see also Merabet *et al.* (Merabet *et al.*, 2000)], would not have been fully expressed, yielding comparable responses whether the optic flow display covered most of the visual field or only the RF. Moreover, the fact that neuronal discharges were not reduced in the presence of large optic flow fields extending beyond the RF is in accord with the real situation observed during locomotion, which is characterized by the expansion of the whole visual field.

Influence of Optic Flow Cues

For centrally located RFs, the removal of size and speed gradients did not strongly affect the response strength nor the direction

selectivity of most PMLS cells. In agreement with our findings, Mulligan *et al.* (Mulligan *et al.*, 1997) have shown that LS cells having centrally located RFs could not distinguish between a single bar moving either at a constant velocity or with acceleration. Comparable findings were reported in the macaque's area MST (Tanaka *et al.*, 1989; Orban *et al.*, 1995). In addition, LS cells were not sensitive to size gradients because their responses were similar whether the single bar was expanding or had a constant size (Mulligan *et al.*, 1997). The inability of centrally located RFs to code for gradient cues may be related to their relatively small surface. The change in size or velocity occurring within the RF would be too small to be meaningful for these units. However, some of our data does not support this assumption since large RFs (up to 1120 degree^2) mapped within 40° of eccentricity were not sensitive to optic flow cues.

A different tendency was observed for the peripherally located RFs. Our data indicate that the removal of gradient cues may strongly affect the response strength and to some extent the direction selectivity of many cells recorded in the anterior part of PMLS cortex. This was especially true for the acceleration component, the effect being more pronounced with increasing velocity. This observation relates well to the characteristics of radial optic flow fields normally encountered during forward locomotion, because changes in perceived velocity and element sizes are more pronounced in the periphery of the visual field. Peripherally located RFs were, on average, larger than those at the center of the visual field, and were therefore more suitable for encoding size changes in the elements. Nevertheless, these behaviorally relevant differences between neuronal responses observed at the center and periphery of the visual field might reflect specialization of the PMLS cortex in visual analysis during self-motion.

Functional Considerations

A functional dichotomy within the PMLS cortex with regards to optic flow processing was also previously suggested on the basis of differences between axial directions of cells in the anterior (centrifugal directions) and posterior (directional preferences orthogonal to optic flow directions) parts of the LS cortex (Sherk *et al.*, 1995). We also propose that such a dichotomy exists along the antero-posterior axis, but the dichotomy is based on receptive field location.

Neurons with centrally located RFs in the posterior part of the PMLS were not strongly sensitive to optic flow cues and responded preferentially to forward motion whether the origin of motion was within the RF or at the area centralis. Given these properties, it is reasonable to propose that the function of these neurons is to indicate that locomotion is initiated and that the animal is heading toward a specific point in the environment (a 'GO' signal). The observation that cells with centrally located RFs could respond to the pattern when the origin of motion was within the RF may be of importance to keep track of the heading point when eye movements (i.e. shifts of gaze) are made and heading line is kept constant. This reference point would still be perceived by these neurons.

Cells in the anterior part of PMLS cortex with peripheral RFs would be stimulated when the animal moves forward. Our study showed that almost all these units were not selective to the direction of optic flow patterns when the origin of motion was within their RF, despite their large size. However, these neurons responded preferentially when the element motion originated from the area centralis, and most were sensitive to cues such as acceleration. While we found a relationship between axial and optic flow direction preferences for most cells, there was a clear mismatch between both directions for a number a PMLS units: so it is possible that part of the mechanisms subtending the coding of optic flow fields are more complex than those involved in the coding of a single stimulus of constant size and velocity moving in pure translation (Tanaka, 1998). One possibility may be that the selectivity of cells representing the periphery of the visual field arises from prior activation (through intrinsic intracortical connections) of the neighboring cells serially linked to the units representing the central part of the visual field. Two findings are in agreement with this last assumption. First, we showed that the responses are more robust in the presence of a speed gradient. Since velocity preference in PMLS cortex increases with eccentricity [(Rauschecker *et al.*, 1987); see Fig. 3 of the present study], it is likely that accelerating elements would cross all receptive fields (being progressively more eccentric) at their optimal speed and would therefore evoke maximal discharges. This would not be possible for elements of constant velocity. Second, we found that response strength and direction selectivity to optic flow patterns were markedly reduced for four of eight expansion-selective cells with peripherally located RFs, when the visual field covering the region from the area centralis to the proximal boundary of the RF was progressively masked (artificial scotoma). This effect was observed despite the fact that the RF was equally stimulated with or without the scotoma (preliminary data, not shown). It is worth pointing out that a high proportion of peripherally located optic flow sensitive cells were located in layers II–III where cortico-cortical connections predominate. These data obviously are preliminary and we must be cautious in our interpretations. Nonetheless, our overall findings suggest that long-range intracortical processing between centrally and peripherally located PMLS RFs may be necessary for the coding of large and cue-rich optic flow fields.

Notes

We are grateful to A. Herbert and C. Habak for helpful comments in the preparation of this manuscript. This work was supported by CIHR (grant #MOP-13359) to C.C. and FCAR. Part of C.C.'s salary was provided by FRSQ. O.B.L. was supported in part by a fellowship from FRSQ–FCAR Santé.

Address correspondence to Christian Casanova, Laboratoire des Neurosciences de la Vision, École d'optométrie, Université de Montréal, CP 6128, succ. Centre-ville, Montréal, Québec, Canada. Email: christian.casanova@umontreal.ca; http://www.mapageweb.umontreal.ca/casanovc/.

References

Akase E, Inokawa H, Toyama K. (1998) Neural responsiveness to three-dimensional motion in cat posteromedial lateral suprasylvian cortex. Exp Brain Res 122:214–226.

Anderson KC, Siegel RM (1999) Optic flow sensitivity in the anterior superior temporal polysensory area, STPa, of the behaving monkey. J Neurosci 19:2681–2692.

Bishop PO, Kozak W, Vakkur GJ (1962) Some quantitative aspects of the cat's eye: axis and plane of reference, visual field coordinates and optics. J Physiol (Lond) 163:466–502.

Blakemore C, Zumbroich TJ (1987) Stimulus selectivity and functional organization in the lateral suprasylvian visual cortex of the cat. J Physiol (Lond) 389:569–603.

Brosseau-Lachaine O, Alarcon M, Lachapelle P, Faubert J, von Grünau MW, Casanova C (1998) Motion analysis in the cat's PMLS cortex: responses to optic flow stimuli. Soc Neurosci Abstr 24:650.

Brosseau-Lachaine O, Filali M, Ptito M, Faubert J, Casanova C (1999) Are optic flow cues for neurons in the cat PMLS cortex similar across the visual field? Soc Neurosci Abstr 25:671.

Camarda R, Rizzolatti G (1976) Visual receptive fields in the lateral suprasylvian area (Clare Bishop area) of the cat. Brain Res 101:427–443.

Dreher B, Djavadian RL, Turlejski KJ, Wang C (1996) Areas PMLS and 21a

of cat visual cortex are not only functionally but also hodologically distinct. Prog Brain Res 112:251–276.
Duffy CJ, Wurtz RH (1991a) Sensitivity of MST neurons to optic flow stimuli. I. A continuum of responses selectivity to large field stimuli. J Neurophysiol 65:1329–1345.
Duffy CJ, Wurtz RH (1991b) Sensitivity of MST neurons to optic flow stimuli. II. Mechanisms of response selectivity revealed by small-field stimuli. J Neurophysiol 65:1346–1359.
Gibson JJ (1950) The perception of the visual world. Boston: Houghton Mifflin.
Gizzi MS, Katz E, Movshon JA (1990a) Spatial and temporal analysis by neurons in the representation of the central visual field in the cat's lateral suprasylvian visual cortex. Vis Neurosci 5:463–468.
Gizzi MS, Katz E, Schumer RA, Movshon JA (1990b) Selectivity for orientation and direction of motion of single neurons in cat striate and extrastriate visual cortex. J Neurophysiol 63:1529–1543.
Goslow GE Jr, Reinking RM, Stuart DG (1973) The cat step cycle: hind limb joint angles and muscle lengths during unrestrained locomotion. J Morphol 141:1–42.
Halbertsma JM (1983) The stride cycle of the cat: the modelling of locomotion by computerized analysis of automatic recordings. Acta Physiol Scand Suppl 521:1–75.
Hamada T (1987) Neuronal response to the motion of textures in the lateral suprasylvian area of cats. Behav Brain Res 25:175–185.
Kim JN, Mulligan K, Sherk H (1997) Simulated optic flow and extrastriate cortex. I. Optic flow versus texture. J Neurophysiol 77:554–561.
Krüger K, Kiefer W, Groh A (1993) Lesion of the suprasylvian cortex impairs depth perception of cats. NeuroReport 4:883–886.
Lagae L, Maes H, Raiguel S, Xiao D, Orban GA (1994) Responses of macaque STS neurons to optic flow components: a comparison of areas MT and MST. J Neurophysiol 71:1597–1626.
Li B, Li BW, Chen Y, Wang LH, Diao YC (2000) Response properties of PMLS and PLLS neurons to stimulated optic flow patterns. Eur J Neurosci 12:1534–1544.
Merabet L, Minville K, Ptito M, Casanova C (2000) Responses of neurons in the cat posteromedial lateral suprasylvian cortex to moving texture patterns. Neuroscience 97:611–623.
Minville K, Casanova C (1998) Spatial frequency processing in the posteromedial lateral suprasylvian cortex does not depend on the projections from the striate-recipient zone of the cat's lateral posterior–pulvinar complex. Neuroscience 84:699–711.
Morrone MC, Di Stephano M, Burr DC (1986) Spatial and temporal properties of neurons of the lateral suprasylvian cortex of the cat. J Neurophysiol 56:969–986.
Mulligan K, Kim JN, Sherk H (1997) Simulated optic flow and extrastriate cortex. II. Response to bar versus large field stimuli. J Neurophysiol 77:562–570.
Orban GA (1984) Neuronal operations in the visual cortex. Berlin: Springer-Verlag.
Orban GA, Lagae L, Verri A, Raiguel S, Xiao D, Maes H, Torre V (1992) First-order analysis of optical flow in monkey brain. Proc Natl Acad Sci USA 89:2595–2599.
Orban GA, Lagae L, Raiguel S, Xiao D, Maes H (1995) The speed tuning of middle superior temporal (MST) cell responses to optic flow components. Perception 24:269–285.
Palmer LA, Rosenquist AC, Tusa RJ (1978) The retinotopic organization of lateral suprasylvian visual areas in the cat. J Comp Neurol 177: 237–256.
Pettigrew JD, Cooper ML, Blasdel GG (1979) Improved use of tapetal reflection for eye-position monitoring. Invest Ophthalmol Vis Sci 18:490–495.
Rauschecker JP, von Grünau MW, Poulin C (1987) Centrifugal organization of direction preferences in the cat's lateral suprasylvian visual cortex and its relation to flow field processing. J Neurosci 7:943–958.
Saito H, Yukie M, Tanaka M, Hikosaka K, Fukada Y, Iwai E (1986) Integration of direction signals of image motion in the superior temporal sulcus of the macaque monkey. J Neurosci 6:145–157.
Sherk H, Mulligan KA (1993) A reassessment of the lower visual field map in striate-recipient lateral suprasylvian cortex. Vis Neurosci 10:131–158.
Sherk H, Kim JN, Mulligan K (1995) Are the preferred directions of neurons in cat extrastriate cortex related to optic flow? Vis Neurosci 12:887–894.
Sherk H, Mulligan K, Kim JN (1997) Neural responses in extrastriate cortex to objet in optic flow fields. Vis Neurosci 14:879–895.
Siegel RM, Read HL (1997) Analysis of optic flow in the monkey parietal area 7a. Cereb Cortex 7:327–346.
Smith JL, Chung SH, Zernicke RF (1993) Gait-related motor patterns and hindlimb kinetics for the cat trot and gallop. Exp Brain Res 94: 308–322.
Spear PD, Baumann TP (1975) Receptive-field characteristics of single neurons in lateral suprasylvian visual area of the cat. J Neurophysiol 38:1403–1420.
Spear PD, Miller S, Ohman L (1983) Effects of lateral suprasylvian visual cortex lesions on visual localization, discrimination, and attention in cats. Behav Brain Res 10:339–359.
Tanaka K (1998) Representation of visual motion in the extrastriate visual cortex. In: High level motion processing. Cambridge: MIT Press.
Tanaka K, Fukuda Y, Saito HA (1989) Underlying mechanisms of the response specificity of expansion/contraction and rotation cells in the dorsal part of the medial superior temporal area of the macaque monkey J Neurophysiol 62:642–656.
Tanaka K, Saito H (1989) Analysis of motion of the visual field by direction, expansion/contraction, and rotation cells clustered in the dorsal part of the medial superior temporal area of the macaque monkey. J Neurophysiol 62:626–641.
Toyama K, Komatsu Y, Kasai H, Fujii K, Umetani K (1985) Responsiveness of Clare–Bishop neurons to visual cues associated with motion of a visual stimulus in three-dimensional space. Vis Res 25:407–414.
Toyama K, Kozasa T (1982) Responses of Clare–Bishop neurons to three dimensional movement of a light stimulus. Vis Res 22:571–574.
von Grünau MW, Frost BJ (1983) Double-opponent process mechanism underlying RF-structure of directionally specific cells of cat lateral suprasylvian visual area. Exp Brain Res 49:84–92.